Semi-empirical PM3 calculation reveals the relationship between the fluorescence characteristics of 4,7-disubstituted benzofurazan compounds, the LUMO energy and the dipole moment directed from the 4- to the 7-position

Seiichi Uchiyama, Tomofumi Santa and Kazuhiro Imai *

Graduate School of Pharmaceutical Sciences, The University of Tokyo, 7-3-1 Hongo, Bunkyo-ku, Tokyo 113-0033, Japan

Received (in Cambridge) 15th October 1998, Accepted 5th January 1999

This article elucidates the relationships between the chemical structure and the fluorescence characteristics (fluorescence intensity, maximum excitation wavelength and maximum emission wavelength) of 4,7-disubstituted benzofurazan compounds with computer calculation. Our previous study using Hammett substituent constants of the substituent groups at the 4- and the 7-positions suggested that the total of electron densities on the benzofurazan skeleton and the dipole moment directed from the 4- to the 7-position might affect the fluorescence characteristics of these compounds. The sum of atomic charges on the benzofurazan skeleton, the HOMO energy and the LUMO energy were selected as parameters to reflect the total of electron densities on the benzofurazan skeleton and were obtained with the AM1 and PM3 calculations. The dipole moment directed from the 4- to the 7-position was also calculated with two hamiltonians. The LUMO energy and the dipole moment from the 4- to the 7-position obtained with the PM3 calculation is most closely related with the fluorescence characteristics. Using these parameters, the fluorescent 4,7-disubstituted benzofurazan compounds were classified into two groups, and the maximum excitation and emission wavelengths were different between these two groups. These relationships indicated that the fluorescence characteristics of 4,7-disubstituted benzofurazan compounds were determined by the total of electron densities on the benzofurazan skeleton and the dipole moment directed from the 4- to the 7-position. Furthermore, we predicted the fluorescence characteristics of four 4,7-disubstituted benzofurazan compounds based on the relationships obtained, and confirmed that the prediction agreed with the measured data.

Introduction

Fluorometric detection has often been adopted in high-performance liquid chromatography (HPLC) because of its sensitivity and selectivity. However, most analytes do not fluoresce, thus, derivatization or chemical transformation of the analytes have to be carried out with various fluorescent derivatization reagents to make the detection method useful for a much wider range of analytes.

For this purpose, various fluorescent derivatization reagents have been developed[1,2] and these can be classified into two categories. One is a "fluorescent tagging or labeling reagent" composed of a highly fluorescent moiety and tagging moiety which reacts with the functional group of analytes to form fluorescent-tagging derivatives. The other is a "fluorogenic reagent" which is non-fluorescent itself and reacts with the analytes to form the fluorescent derivatives. The fluorogenic reagents are generally superior to the fluorescent tagging or labeling reagents, since the fluorogenic reagents avoid interference from the fluorescence of reagents themselves. The following compounds have so far been reported to be typical fluorogenic reagents: 5-(dimethylamino)napthalene-1-sulfonyl chloride (Dns-Cl),[3] 5-di(*n*-butylamino)naphthalene-1-sulfonyl chloride (Bns-Cl),[4] 4-chloro-7-nitro-2,1,3-benzoxadiazole (NBD-Cl),[5] 4-fluoro-7-nitro-2,1,3-benzoxadiazole (NBD-F),[6] 4-(*N*,*N*-dimethylaminosulfonyl)-7-fluoro-2,1,3-benzoxadiazole (DBD-F),[7] 4-aminosulfonyl-7-fluoro-2,1,3-benzoxadiazole (ABD-F),[8] 7-fluoro-2,1,3-benzoxadiazole-4-sulfonate (SBD-F),[9] 4′-phenylspiro[2-benzofuran-3,2′-furan]-1(3*H*),3′(2*H*)-dione (fluorescamine),[10] 2-methoxy-2,4-diphenylfuran-3(2*H*)-one (MDPF)[11] and *o*-phthalaldehyde (OPA).[12]

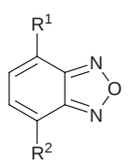

Fig. 1 Chemical structure of 4,7-disubstituted benzofurazan compounds (R^1, R^2; substituent groups).

Although there have been many reports on the effects of the chemical structure or substituent groups[13–18] on the fluorescence characteristics of the molecules (fluorescence intensity, maximum excitation and emission wavelengths), there is no general rule that can predict the fluorescence characteristics of the objective molecule accurately from its chemical structure. To develop a new sensitive fluorogenic reagent, the establishment of a general rule is necessary. In our previous report,[19] we investigated the effects of the substituent groups of the 4,7-disubstituted benzofurazan (2,1,3-benzoxadiazole) compounds (Fig. 1) on the fluorescence characteristics and found the relationship between the fluorescence characteristics, the sum and the difference of the Hammett substituent constants (σp)[20–22] of substituent groups at the 4- and 7-positions. Furthermore the usefulness of the relationship was demonstrated through the development of a new fluorogenic reagent for amines. However, the reason why the sum and the difference of the Hammett substituent constants are related to the fluorescence characteristics is still obscure and the applicability of the rule is limited to the benzofurazan compounds having substituent groups with known Hammett substituent constants.

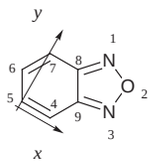

Fig. 2 Position number of the benzofurazan skeleton and coordinate axes assigned to the computer calculation of the dipole moment. The *X* and *Y* axes were defined by semi-empirical calculation program soft WinMOPAC ver. 1.0 automatically.

In this article, we try to solve these problems. The sum and the difference of Hammett substituent constants seem to correspond to the electron richness or poorness on the benzofurazan skeleton and the polarization from the 4- to the 7-position respectively. Therefore, the total of the electron densities on the benzofurazan skeleton and the dipole moment directed from the 4- to 7-position were expected to relate to the fluorescence characteristics of the 4,7-disubstituted benzofurazan compounds. The sum of atomic charges on the benzofurazan skeleton, the HOMO energy and the LUMO energy were adopted as parameters to reflect the total electron densities on the benzofurazan skeleton and were calculated with the AM1[23] and the PM3,[24,25] semi-empirical molecular orbital calculations. The dipole moment directed from the 4- to the 7-position was also calculated with two hamiltonians. We investigated the relationship between these parameters and the fluorescence characteristics of 4,7-disubstituted benzofurazan compounds and selected the parameter suitable to give the best relationship. Also, we described the prediction for the fluorescence characteristics of 4,7-disubstituted benzofurazan compounds based on the best relationship.

Results and discussion

The relationship between the fluorescence characteristics and the chemical structure of 4,7-disubstituted benzofurazan compounds

Sixty-eight 4,7-disubstituted benzofurazan compounds, denoted R^1/R^2 in the text with the substituent groups at the 4- and the 7-positions (R^1 and R^2), were investigated in this work. The substituent groups, the relative fluorescence intensity, the maximum excitation wavelengths and the maximum emission wavelengths of these compounds in methanol are summarized in Table 1. The fluorescence spectra of the new benzofurazan compounds (No. 32, 39, 41, 43, 53 and 63) were measured in this study, while those of the others were taken from our previous report.[19]

To elucidate the relationship between the fluorescence characteristics and the chemical structure of 4,7-disubstituted benzofurazan compounds, the parameters best suited to represent the electronic status of the benzofurazan skeleton should be selected. In our previous paper,[19] we reported that the sum and the difference of the Hammett substituent constants (σ_p) at the 4- and 7-positions were related to the fluorescence characteristics. These results suggested that the total of electron densities on the benzofurazan skeleton and the dipole moment from the 4- to 7-position of the benzofurazan skeleton were related to the fluorescence intensity. Therefore, the total of electron densities on the benzofurazan skeleton and the dipole moment from the 4- to the 7-position of benzofurazan skeleton were selected and obtained with the AM1[23] and the PM3[24,25] semi-empirical molecular orbital calculations in this study.

The total of electron densities on the benzofurazan skeleton cannot be obtained directly with the AM1 and the PM3 methods. Therefore, at first, we used the sum of atomic charges on the benzofurazan skeleton for the total of electron densities on the benzofurazan skeleton, the total of the charge on oxygen, nitrogen and carbon atoms in the benzofurazan skeleton, calculated according to eqn. (1). The dipole moment

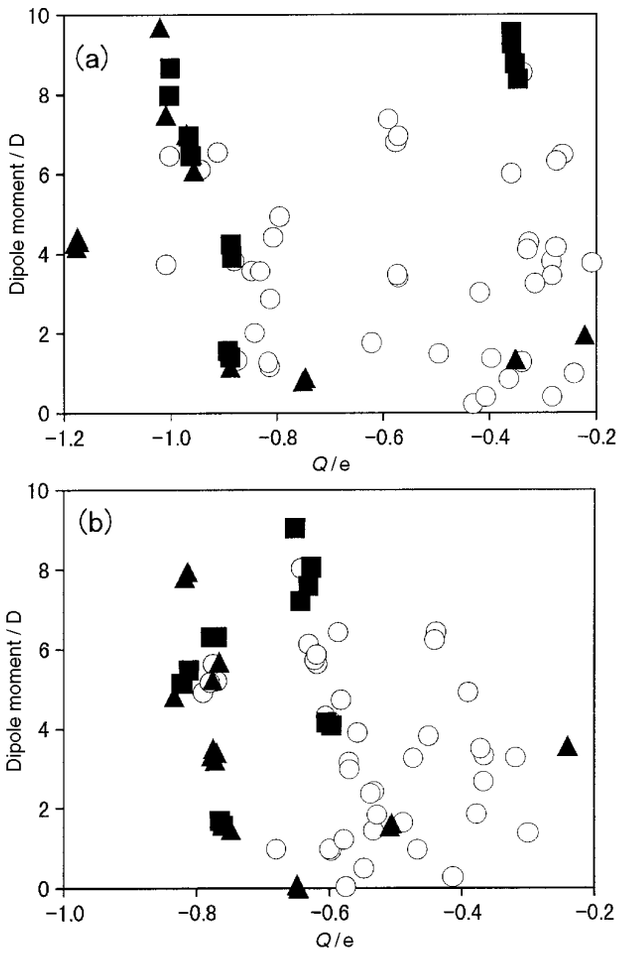

Fig. 3 The relationship between the sum of atomic charges on the benzofurazan skeleton (*Q*), the dipole moment from the 4- to the 7-position calculated with AM1 (a) and PM3 (b) methods and the relative fluorescence intensity (RFI) of benzofurazan compounds; ■, RFI ≥ 5.0; ▲, 5.0 > RFI ≥ 1.0; ○, 1.0 > RFI.

from the 4- to the 7-position was obtained by the projection of two vectors obtained with computer calculation (Fig. 2) to the axis directed from the 4- to the 7-position of the benzofurazan skeleton according to eqn. (2). These values are summarized in Table 1.

$$\text{Sum of the charges } (Q)/\text{e} = q[\text{N1}] + q[\text{O2}] + q[\text{N3}] + q[\text{C4}] + q[\text{C5}] + q[\text{C6}] + q[\text{C7}] + q[\text{C8}] + q[\text{C9}] \quad (1)$$

$$\text{Dipole moment directed from 4- to 7-position/D} = |\text{dipole moment } (x) \times \cos(\varphi\,[\text{C(7)–C(4)–C(5)}]) - \text{dipole moment } (y) \times \sin(\varphi[\text{C(7)–C(4)–C(5)}])| \quad (2)$$

To simplify the relationship between the chemical structure and the fluorescence intensity, the benzofurazan compounds were classified into three groups according to their relative fluorescence intensity (RFI = 0–1, having no or weak fluorescence; RFI = 1–5, having moderate fluorescence; RFI > 5, having strong fluorescence). Fig. 3 shows the relationships between the sum of atomic charges on the benzofurazan skeleton, the dipole moment from the 4- to the 7-position calculated with the AM1 and the PM3 methods and the relative fluorescence intensity of sixty-eight benzofurazan compounds. No correlation was observed among these parameters as shown in Fig. 3.

Next, instead of the sum of atomic charges on the benzofurazan skeleton, the HOMO (highest occupied molecular

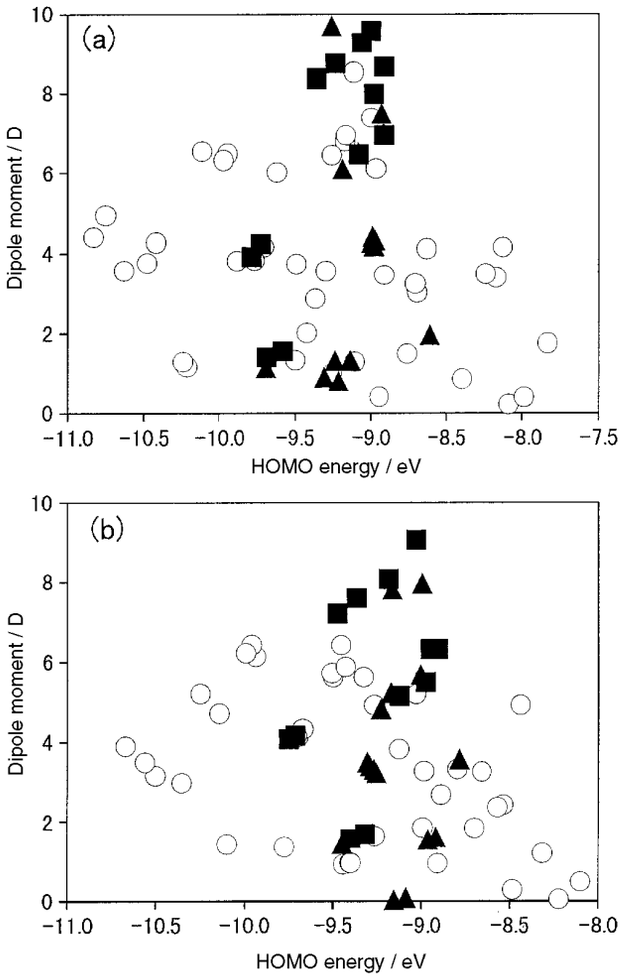

Fig. 4 The relationship between the HOMO energy, the dipole moment from the 4- to the 7-position calculated with AM1 (a) and PM3 (b) methods and the relative fluorescence intensity (RFI) of benzofurazan compounds; ■, RFI ⩾ 5.0; ▲, 5.0 > RFI ⩾ 1.0; ○, 1.0 > RFI.

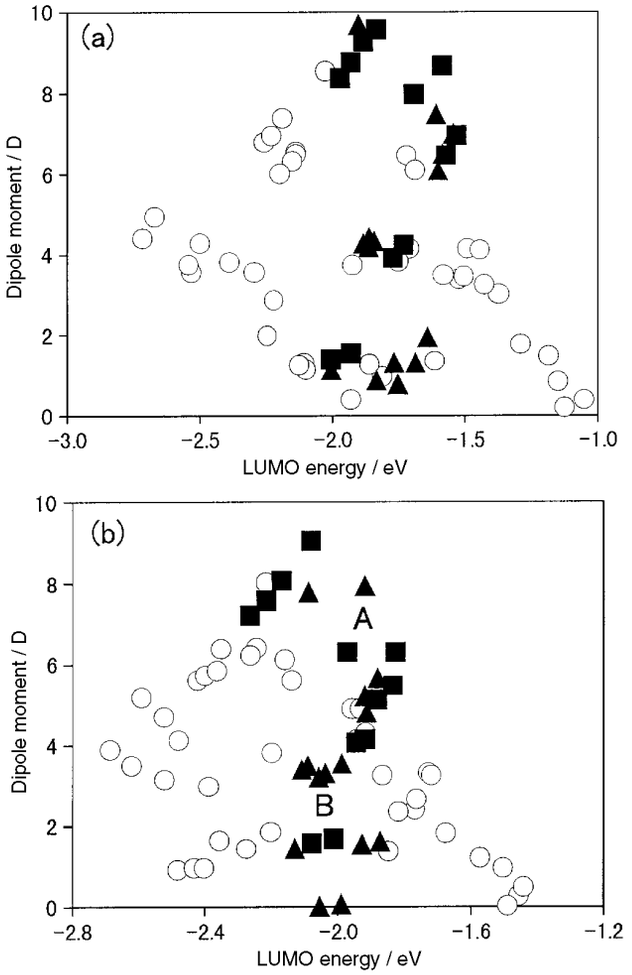

Fig. 5 The relationship between the LUMO energy, the dipole moment from the 4- to the 7-position calculated with AM1 (a) and PM3 (b) methods and the relative fluorescence intensity (RFI) of benzofurazan compounds; ■, RFI ⩾ 5.0; ▲, 5.0 > RFI ⩾ 1.0; ○, 1.0 > RFI.

orbital) energy (Table 1) was adopted. Because the greater part of the electron in the HOMO calculated with the AM1 and the PM3 methods is distributed on the benzofurazan skeleton, the HOMO energy seems to reflect the total of electron densities on the benzofurazan skeleton. Fig. 4 shows the relationships among the HOMO energy, the dipole moment from the 4- to the 7-position calculated with the AM1 and the PM3 methods and the relative fluorescence intensity of the sixty-eight benzofurazan compounds. As shown in Fig. 4, the fluorescent compounds, represented as closed squares and closed triangles, were concentrated more as compared with the case using the sum of the charges on the benzofurazan skeleton.

Finally, the LUMO (lowest unoccupied molecular orbital) energy (Table 1), as another value to reflect the total of electron densities on the benzofurazan skeleton, was adopted. The greater part of the electron in the LUMO calculated with the AM1 and the PM3 methods was also distributed on the benzofurazan skeleton. Hence the LUMO seems to reflect the total of electron densities on the benzofurazan skeleton, too. The relationships between the LUMO energy, the dipole moment from the 4- to the 7-position calculated with the AM1 and the PM3 methods and the relative fluorescence intensity of sixty-eight benzofurazan compounds are shown in Fig. 5. The fluorescent benzofurazan compounds were concentrated in two areas (areas A and B, named for convenience) using the LUMO energy obtained with the PM3 method (Fig. 5(b)) as a parameter, in contrast, the non-fluorescent benzofurazan compounds scattered out of these two areas.

These results suggest that the PM3 method was more suitable than the AM1 to evaluate the relationships between the total of electron densities on the benzofurazan skeleton and the dipole moment directed from the 4- to the 7-position. The benzofurazan skeleton includes nitrogen and oxygen atoms and the substituent groups also include nitrogen, oxygen, fluorine, chlorine and sulfur atoms. Therefore the PM3 method, which can calculate the electronic states of the compounds including these atoms more accurately,[26,27] gave good results, compared with the AM1 method.

The LUMO energy was the most appropriate to represent the total of electron densities on benzofurazan skeleton. Semi-empirical AM1 and PM3 methods could not calculate precisely the charge of the various kinds of atoms in 4,7-disubstituted benzofurazan compounds. The use of the LUMO energy gave better results than the use of the HOMO energy, because the electron in the LUMO obtained with the PM3 method was distributed on the benzofurazan skeleton more than the electron in the HOMO and thus the LUMO can reflect the total of electron densities on the benzofurazan skeleton more precisely. These results were in agreement with the report,[28] in which the PM3 method gave the best results in the calculation of the acidity of 4-substituted benzoic acids.

The grouping of the plots of the fluorescent 4,7-disubstituted benzofurazan compounds in Fig. 5(b) indicates that the fluorescence intensity of the 4,7-disubstituted benzofurazan compounds is determined by both the total of electron densities on the benzofurazan skeleton and the dipole moment directed

Table 1 Substituent groups, fluorescence characteristics and molecular parameters, computed by AM1 and PM3 methods, of 4,7-disubstituted benzofurazan compounds

							AM1				PM3			
No.	R^1	R^2	Ref	RFI[a]	λ (ex.)/nm	λ (em.)/nm	*Q*/e[b]	*E*(HOMO)/eV	*E*(LUMO)/eV	DM (4–7)/D[c]	*Q*/e[b]	*E*(HOMO)/eV	*E*(LUMO)/eV	DM (4–7)/D[c]
1	SO_2Ph	NHCOPh	19	172.6	368	492	−0.891	−9.581	−1.929	1.540	−0.764	−9.318	−2.012	1.675
2	SO_2Ph	NHAc	19	84.4	366	486	−0.888	−9.686	−2.004	1.389	−0.760	−9.398	−2.076	1.555
3	NO_2	NHMe	19	62.7	467	528	−0.352	−9.234	−1.931	8.748	−0.631	−9.364	−2.215	7.577
4	NO_2	NH_2	19	54.5	460	532	−0.346	−9.354	−1.971	8.359	−0.643	−9.471	−2.264	7.204
5	SO_2NMe_2	NPr^n_2	19	8.8	459	563	−1.000	−8.909	−1.586	8.652	−0.770	−8.902	−1.826	6.304
6	SO_2NH_2	OEt	19	7.9	353	471	−0.887	−9.722	−1.728	4.232	−0.604	−9.709	−1.918	4.151
7	NO_2	NMe_2	17	7.2	481	533	−0.358	−9.058	−1.881	9.257	−0.626	−9.183	−2.168	8.056
8	SO_2NMe_2	NMe_2	7	6.7	448	563	−0.966	−8.908	−1.531	6.946	−0.812	−8.969	−1.833	5.470
9	SO_2NHPh	NMe_2	19	6.7	449	562	−1.003	−8.974	−1.694	7.966	−0.778	−8.947	−1.971	6.302
10	SO_2NH_2	OMe	19	6.0	352	468	−0.883	−9.785	−1.771	3.902	−0.596	−9.746	−1.945	4.068
11	SO_2NMe_2	NHMe	19	5.9	430	552	−0.963	−9.076	−1.571	6.450	−0.822	−9.118	−1.882	5.131
12	NO_2	NPr^n**2**	19	5.2	489	538	−0.358	−8.996	−1.836	9.546	−0.651	−9.027	−2.079	9.036
13	SO_2NH_2	NPr^n_2	19	4.9	459	573	−1.009	−8.929	−1.609	7.483	−0.813	−8.993	−1.919	7.952
14	SO_2NH_2	SMe	19	4.2	385	511	−1.181	−8.993	−1.885	4.275	−0.770	−9.291	−2.109	3.398
15	SO_2NH_2	SEt	19	3.4	387	511	−1.175	−8.987	−1.862	4.421	−0.775	−9.303	−2.091	3.500
16	Cl	NHCOPh	19	3.1	366	520	−0.352	−9.136	−1.686	1.318	−0.506	−8.915	−1.873	1.613
17	SO_2NH_2	NMe_2	19	2.9	448	570	−0.970	−8.916	−1.544	6.997	−0.766	−9.002	−1.880	5.674
18	SO_2NMe_2	SMe	19	2.8	390	507	−1.177	−8.979	−1.865	4.180	−0.772	−9.252	−2.056	3.213
19	SO_2NMe_2	NHAc	19	2.4	369	492	−0.888	−9.692	−2.004	1.139	−0.748	−9.447	−2.130	1.449
20	SO_2NMe_2	SEt	19	2.3	393	508	−1.173	−8.973	−1.843	4.328	−0.778	−9.265	−2.038	3.311
21	Cl	NHAc	19	2.1	368	521	−0.350	−9.238	−1.766	1.317	−0.509	−8.963	−1.928	1.551
22	SO_2NH_2	NHMe	19	2.0	430	563	−0.960	−9.086	−1.585	6.509	−0.776	−9.170	−1.919	5.229
23	SOPh	NHCOPh	19	1.9	368	506	−0.751	−9.214	−1.754	0.787	−0.649	−9.085	−1.989	0.083
24	SO_2F	NMe_2	7	1.6	440	533	−1.020	−9.259	−1.902	9.685	−0.818	−9.164	−2.089	7.803
25	SOPh	NHAc	19	1.6	369	506	−0.747	−9.308	−1.833	0.881	−0.646	−9.152	−2.055	0.022
26	NCS	OMe	17	1.4	384	523	−0.221	−8.610	−1.642	1.951	−0.240	−8.781	−1.987	3.555
27	SO_2NMe_2	NH_2	33	1.0	428	559	−0.957	−9.186	−1.602	6.094	−0.834	−9.228	−1.913	4.820
28	SPh	NHCOPh	19	0.8	400	559	−0.571	−8.169	−1.521	3.383	−0.532	−8.533	−1.768	2.410
29	SO_2Cl	F	8	0.7	352	459	−0.807	−10.829	−2.717	4.413	−0.557	−10.672	−2.684	3.887
30	F	NHAc	19	0.6	363	520	−0.241	−9.255	−1.811	0.964	−0.319	−8.982	−1.865	3.265
31	NO_2	SMe	19	0.6	427	507	−0.576	−9.172	−2.257	6.787	−0.618	−9.496	−2.421	5.614
32	SO_2F	F	new	0.5	331	453	−0.847	−10.628	−2.532	3.561	−0.570	−10.502	−2.521	3.145
33	SPh	NHAc	19	0.5	392	554	−0.573	−8.240	−1.582	3.478	−0.537	−8.567	−1.817	2.357

34	NO_2	NHAc	19	0.4	416	503	−0.283	−9.883	−2.390	3.806	−0.596	−9.693	−2.479	4.117
35	SO_2NH_2	NH_2	33	0.4	424	568	−1.001	−9.256	−1.719	6.444	−0.790	−9.264	−1.958	4.909
36	NO_2	SEt	19	0.3	428	495	−0.571	−9.163	−2.231	6.935	−0.622	−9.504	−2.399	5.716
37	SO_2NH_2	NCS	33	0.3	356	475	−0.831	−9.295	−2.295	3.552	−0.597	−9.441	−2.482	0.911
38	SO_2NMe_2	OEt	19	0.2	353	469	−0.885	−9.705	−1.709	4.149	−0.605	−9.671	−1.917	4.315
39	Cl	NHCSOMe	new	0.2	380	521	−0.338	−9.103	−1.859	1.270	−0.450	−9.123	−2.198	3.807
40	NCS	Cl	17	0.1	416	519	−0.281	−8.942	−1.928	0.392	−0.378	−8.989	−2.202	1.843
41	H	NMe_2	new	0.1	430	589	−0.495	−8.757	−1.183	1.477	−0.467	−8.907	−1.502	0.954
42	NHAc	OMe	19	0.1	416	540	−0.281	−8.909	−1.503	3.447	−0.366	−8.794	−1.727	3.313
43	SO_2Cl	Cl	34	0.0			−0.794	−10.751	−2.671	4.934	−0.769	−10.247	−2.591	5.186
44	SO_2F	OPh	35	0.0			−0.911	−10.114	−2.137	6.541	−0.631	−9.933	−2.159	6.128
45	NO_2	Cl	5	0.0			−0.325	−10.418	−2.501	4.275	−0.582	−10.142	−2.522	4.703
46	NO_2	SPh	19	0.0			−0.590	−8.993	−2.189	7.375	−0.619	−9.427	−2.364	5.855
47	NO_2	F	36	0.0			−0.207	−10.474	−2.541	3.752	−0.371	−10.560	−2.621	3.492
48	NO_2	OPh	19	0.0			−0.263	−9.945	−2.137	6.484	−0.438	−9.958	−2.245	6.413
49	NO_2	OMe	17	0.0			−0.274	−9.972	−2.152	6.314	−0.441	−9.989	−2.262	6.223
50	NO_2	$NHNH_2$	37	0.0			−0.359	−9.617	−2.197	6.009	−0.586	−9.451	−2.351	6.398
51	NO_2	NHPh	19	0.0			−0.337	−9.112	−2.026	8.532	−0.642	−9.184	−2.216	8.027
52	SO_2NMe_2	NCS	33	0.0			−0.812	−9.366	−2.220	2.862	−0.600	−9.404	−2.433	0.963
53	SO_2NMe_2	NHCOSMe	new	0.0			−0.875	−9.497	−2.106	1.304	−0.679	−9.396	−2.402	0.966
54	SO_2NMe_2	F	7	0.0			−0.814	−10.212	−2.097	1.145	−0.533	−10.096	−2.274	1.428
55	SO_2NHPh	F	19	0.0			−0.841	−9.418	−2.244	1.990	−0.488	−9.262	−2.357	1.635
56	SO_2NMe_2	OMe	19	0.0			−0.880	−9.767	−1.750	3.815	−0.597	−9.706	−1.942	4.154
57	SO_2NMe_2	NHPh	19	0.0			−0.944	−8.965	−1.688	6.092	−0.780	−9.022	−1.883	5.159
58	SO_2NH_2	F	8	0.0			−0.816	−10.238	−2.125	1.263	−0.569	−10.351	−2.388	2.959
59	SO_2NH_2	$NHNH_2$	38	0.0			−1.008	−9.488	−1.924	3.727	−0.775	−9.323	−2.139	5.612
60	NCS	NMe_2	17	0.0			−0.275	−8.123	−1.490	4.141	−0.390	−8.431	−1.932	4.908
61	Cl	NH_2	17	0.0			−0.418	−8.691	−1.372	3.017	−0.527	−8.695	−1.674	1.820
62	SPh	NH_2	19	0.0			−0.621	−7.830	−1.289	1.747	−0.577	−8.312	−1.571	1.204
63	F	H	36	0.0			−0.396	−9.683	−1.613	1.340	−0.300	−9.774	−1.848	1.368
64	F	NH_2	19	0.0			−0.314	−8.708	−1.426	3.244	−0.367	−8.886	−1.763	2.662
65	NHAc	NMe_2	19	0.0			−0.329	−8.629	−1.444	4.104	−0.472	−8.652	−1.719	3.253
66	OMe	NH_2	17	0.0			−0.363	−8.397	−1.149	0.839	−0.413	−8.481	−1.456	0.274
67	NH_2	NH_2	19	0.0			−0.430	−8.086	−1.124	0.206	−0.575	−8.220	−1.488	0.035
68	NH_2	NMe_2	17	0.0			−0.406	−7.987	−1.051	0.379	−0.547	−8.099	−1.440	0.489

[a] RFI = Relative fluorescence intensity of SO_2NMe_2/NH_2 was arbitrarily taken as 1.0. [b] Q = Sum of the atomic charges on carbon, nitrogen and oxygen atoms in the benzofurazan skeleton. [c] DM (4–7) = Dipole moment directed from the 4- to the 7-position.

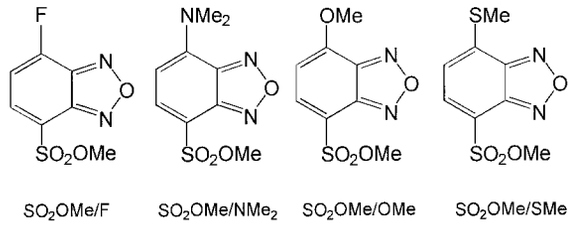

Fig. 6 Chemical structures of four benzofurazan compounds used for the prediction of the fluorescence characteristics.

Table 2 The LUMO energy and the dipole moment directed from the 4- to the 7-position of four benzofurazan compounds obtained with PM3 calculation

R^1	R^2	*E*(LUMO)/eV	DM (4–7)/D[a]
SO_2OMe	F	−2.324	1.408
SO_2OMe	NMe_2	−1.920	5.746
SO_2OMe	OMe	−1.999	4.091
SO_2OMe	SMe	−2.163	3.369

[a] DM (4–7) = Dipole moment directed from the 4- to the 7-position.

from the 4- to the 7-position of the benzofurazan skeleton. The fluorescence occurs with a transition from the lowest vibrational level of the first excited state to any one of the vibrational levels of the ground state. Therefore the calculation of the LUMO energy and the dipole moment directed from the 4- to the 7-position of the chemical structure of the first singlet state may be suitable for investigating the relationship between the chemical structure and the fluorescence intensity. However to calculate these parameters of the excited state with the PM3 method requires too much time and, if calculated, the results obtained might be unreliable. The LUMO energy and the dipole moment directed from the 4- to the 7-position of benzofurazan compounds of the ground state obtained with the PM3 method may reflect those of the first excited state.[18] Therefore employing these values for the ground state is appropriate to elucidate the relationship between the chemical structure and the fluorescence intensity. The reason for the grouping of the plots of the fluorescent benzofurazan compounds cannot be explained theoretically and may be elucidated by further research of the radiationless processes such as the internal conversion and intersystem crossing.

The excitation and the emission wavelengths of the fluorescent benzofurazan compounds plotted in the area A are from 428 to 489 nm and from 528 to 573 nm respectively, while those of the fluorescent benzofurazan compounds plotted in the area B are from 352 to 393 nm and from 468 to 523 nm respectively. The fact that compounds with large dipole moments generally undergo intramolecular charge transfer (ICT)[29–31] in the excited state and are also excited at longer wavelengths[31,32] agrees with the results that the compounds having larger dipole moments in area A have larger excitation and emission wavelengths than the compounds in area B.

The prediction of the fluorescent characteristics of 4,7-disubstituted benzofurazan compounds from their chemical structure

We tried to predict the fluorescence characteristics of the new 4,7-disubstituted benzofurazan compounds shown in Fig. 6, employing the LUMO energy and the dipole moment directed from the 4- to the 7-position (Table 2) calculated with the PM3 method. As shown in Fig. 7, the plot of SO_2OMe/F was out of the fluorescent area, while the plots of SO_2OMe/OMe and SO_2OMe/NMe_2 were in the fluorescent area. Therefore SO_2OMe/F is estimated to be non-fluorescent, while SO_2OMe/OMe and SO_2OMe/NMe_2 were estimated to be fluorescent. SO_2OMe/SMe showed the possibility of being fluorescent, because the plot of SO_2OMe/SMe was on the border between

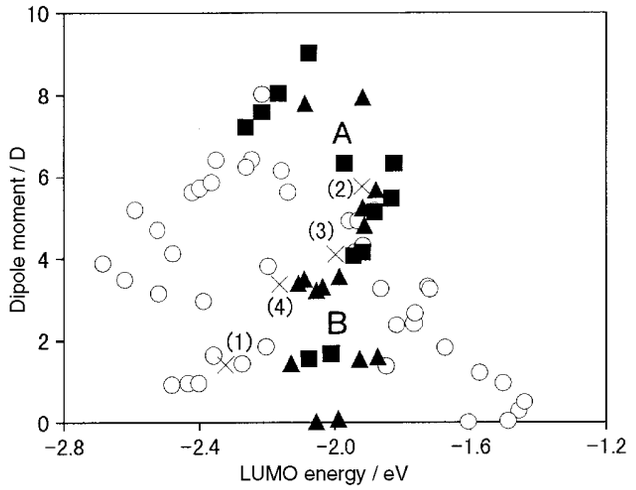

Fig. 7 The plot of four benzofurazan compounds on Fig. 3 for the prediction of the fluorescence characteristics; (1), SO_2OMe/F; (2), SO_2OMe/NMe_2; (3), SO_2OMe/OMe; (4), SO_2OMe/SMe.

Table 3 The fluorescence characteristics of four benzofurazan compounds

R^1	R^2	RFI[a]	λ (ex.)/nm	λ (em.)/nm
SO_2OMe	F	0.0		
SO_2OMe	NMe_2	3.7	441	548
SO_2OMe	OMe	7.1	348	461
SO_2OMe	SMe	1.5	382	504

[a] RFI = Relative fluorescence intensity of SO_2NMe_2/NH_2 was arbitrarily taken as 1.0.

the fluorescent area and the non-fluorescent area. And the plot of SO_2OMe/NMe_2 is in the area A and the plots of SO_2OMe/OMe and SO_2OMe/SMe were in/near the area B respectively, while the maximum excitation and emission wavelengths of the former were estimated to be longer than those of the latter.

The observed results of the fluorescence characteristics of these four 4,7-disubstituted compounds are summarized in Table 3. The predicted fluorescence characteristics of these compounds were in good agreement with those observed. These results suggest that the fluorescence characteristics of 4,7-disubstituted benzofurazan compounds can be predicted from the chemical structure using the LUMO energy and the dipole moment directed from the 4- to the 7-position obtained with the PM3 calculation.

In this study, we demonstrated that the fluorescence characteristics of 4,7-disubstituted benzofurazan compounds were related to the total of electron densities on the benzofurazan skeleton and the dipole moment directed from the 4- to the 7-position, using a semi-empirical PM3 method, elucidating the relationship between the chemical structure and the fluorescence characteristics of all 4,7-disubstituted benzofurazan compounds. The establishment of the procedure to predict the fluorescence characteristics from the chemical structure of 4,7-disubstituted benzofurazan compounds enables the design of fluorogenic compounds like SO_2OMe/F and extends the possibility of the development of further sensitive fluorogenic benzofurazan reagents substituted at the 4- and the 7-positions. These approaches might be applicable to elucidate the relationship between the chemical structures and the fluorescence characteristics of compounds with various kinds of skeletons.

Experimental

Materials

NO_2/Cl (NBD-Cl, No. 45), NO_2/F (NBD-F, No. 47), SO_2NMe_2/F (DBD-F, No. 54) and sodium methanethiolate solution (15%

in water) were obtained from Tokyo Kasei (Tokyo, Japan). Dimethylamine solution (40% in water), triethylamine, dichloromethane, sodium sulfate and hexane were purchased from Kanto Chemicals (Tokyo, Japan). SO_2NH_2/F (ABD-F, No. 58) was obtained from Wako Pure Chemicals (Osaka, Japan). Acetonitrile and methanol were of HPLC grade (Kanto Chemicals, Tokyo, Japan). Water was purified using a Milli-Q reagent system (Millipore, Bedford, MA, USA). All other chemicals were of analytical or guaranteed reagent grade and were used without further purification.

Apparatus

Melting points were measured on a Yanagimoto Micro Melting Point Apparatus (Tokyo, Japan) and uncorrected. Proton nuclear magnetic resonance (^{1}H-NMR) spectra were obtained on a JEOL GSX-400 spectrometer (Tokyo, Japan) with tetramethylsilane as an internal standard in $CDCl_3$ (abbreviations used: s = singlet, d = doublet and m = multiplet), *J* values are given in Hz. Mass spectra were measured on Hitachi M-1200 H mass spectrometer (atomospheric pressure chemical ionization (APCI) system) (Tokyo, Japan). Fluorescence intensity, the maximum excitation wavelength and the maximum emission wavelngth were measured with a Hitachi F-4010 fluorescence spectrometer (Tokyo, Japan) in methanol (5 μM).

Synthesis

4,7-Disubstituted benzofurazan compounds reported previously were obtained according to published procedures (summarized in Table 1), except for NO_2/Cl (No. 45), NO_2/F (No. 47), SO_2NMe_2/F (No. 54) and SO_2NH_2/F (No. 58).

4-Fluorosulfonyl-7-fluoro-2,1,3-benzoxadiazole (SO_2F/F, No. 32). SO_2Cl/F (200 mg, 0.85 mmol, No. 29) and potassium fluoride were dissolved in acetonitrile (2 ml). After the addition of 18-crown-6 ether (15 mg) in acetonitrile (1 ml), the mixture was stirred at room temperature for 8 hours. The reaction mixture was poured into 100 ml of water and extracted with dichloromethane. The organic layer was dried over anhydrous sodium sulfate and concentrated *in vacuo*. The residue was chromatographed on silica gel with ethyl acetate–hexane (1 : 2) to afford SO_2F/F (150 mg, 80%) as a white powder, mp: 72–73 °C. δ_H 8.34 (1H, m), 7.29 (1H, m). Found: C, 32.85; H, 1.20; N, 12.70. Calc. For $C_6H_2F_2N_2O_3S$: C, 32.73; H, 0.92; N, 12.72%; APCI-MS: *m*/*z* 217 ($(M - F + O)^-$) as methanol adduct.

7-Chloro-4-methoxythioamido-2,1,3-benzoxadiazole (Cl/NHCSOMe, No. 39). NCS/Cl (100 mg, 0.47 mmol, No. 40) was dissolved in methanol (20 ml). The mixture was stirred at room temperature for 1 hour. The reaction mixture was evaporated to dryness under reduced pressure, and the residue was chromatographed on silica gel with dichloromethane–hexane (2 : 1) to afford Cl/NHCSOMe (99 mg, 86%) as a yellow powder, mp: 104 °C. δ_H 8.83 (1H, br), 7.41 (1H, d, *J* 8.0), 4.18 (3H, s). Found: C, 39.27; H, 2.60; N, 17.39. Calc. For $C_8H_6ClN_3O_2S$: C, 39.43; H, 2.48; N, 17.24%; APCI-MS: *m*/*z* 242 ($(M - H)^-$).

4-(*N*,*N*-Dimethylamino)-2,1,3-benzoxadiazole (H/NMe_2, No. 41). F/H (100 mg, 0.72 mmol, No. 63) was dissolved in acetonitrile (2 ml). After the addition of dimethylamine solution (300 μl), the mixture was stirred at room temperature for 4 hours. The reaction mixture was evaporated to dryness under reduced pressure, and the residue was chromatographed on silica gel with dichloromethane–hexane (1 : 1) to afford H/NMe_2 (29 mg, 25%) as an orange powder, mp: 34–35 °C. δ_H 7.23 (1H, d, *J* 8.0), 7.06 (1H, d, *J* 8.0), 6.06 (1H, d, *J* 8.0), 3.32 (6H, s). APCI-MS: *m*/*z* 164 ($(M + H)^+$).

7-(*N*,*N*-Dimethylamino)sulfonyl-4-methoxythioamido-2,1,3-benzoxadiazole (SO_2NMe_2/NHCSOMe, No. 53). SO_2NMe_2/NCS (60 mg, 0.21 mmol, No. 52) was dissolved in methanol (10 ml). The solution was stirred at room temperature for 1 hour. The reaction mixture was evaporated to dryness under reduced pressure, and the residue was chromatographed on silica gel with dichloromethane to afford SO_2NMe_2/NHCSOMe (59 mg, 89%) as a yellow powder, mp: 178–179 °C. δ_H 9.04 (1H, d, *J* 8.0), 8.42 (1H, br), 8.04 (1H, d, *J* 8.0), 4.22 (3H, s), 2.94 (6H, s). Found: C, 37.88; H, 4.01; N, 17.86. Calc. For $C_{10}H_{12}N_4O_4S_2$: C, 37.97; H, 3.82; N, 17.71%; APCI-MS: *m*/*z* 315 ($(M - H)^-$).

4-Methoxysulfonyl-7-fluoro-2,1,3-benzoxadiazole (SO_2OMe/F). SO_2Cl/F (158 mg, 0.67 mmol) was dissolved in acetonitrile (5 ml). After the addition of sodium methoxide (53 mg, 0.98 mmol) in methanol (10 ml), the mixture was stirred at room temperature for 10 minutes. The reaction mixture was evaporated to dryness under reduced pressure, and the residue was chromatographed on silica gel with dichloromethane–hexane (1 : 1) to afford SO_2OMe/F (19 mg, 12%) as a white powder, mp: 87 °C. δ_H 8.18 (1H, m), 7.22 (1H, m), 4.05 (3H, s); APCI-MS: *m*/*z* 232 (M^-).

4-(*N*,*N*-Dimethylamino)-7-methoxysulfonyl-2,1,3-benzoxadiazole (SO_2OMe/NMe_2). SO_2OMe/F (4.0 mg, 0.017 mmol) was dissolved in acetonitrile (2 ml). After the addition of dimethylamine solution (10 μl), the mixture was stirred at room temperature for 20 minutes. The reaction mixture was chromatographed on silica gel with dichloromethane to afford SO_2OMe/NMe_2 (3.7 mg, 85%) as a yellow powder, mp: 115–116 °C. δ_H 7.96 (1H, d, *J* 8.0), 6.05 (1H, d, *J* 8.0), 3.88 (3H, s), 3.55 (6H,s); APCI-MS: *m*/*z* 258 ($(M + H)^+$).

4-Methoxy-7-methoxysulfonyl-2,1,3-benzoxadiazole (SO_2OMe/OMe). SO_2OMe/F (20 mg, 0.086 mmol) was dissolved in methanol (20 ml). After the addition of triethylamine (200 μl), the mixture was stirred at 60 °C for 5 hours. The reaction mixture was evaporated to dryness under reduced pressure, and the residue was chromatographed on silica gel with dichloromethane to afford SO_2OMe/OMe (14 mg, 67%) as a white powder, mp: 130–131 °C. δ_H 8.06 (1H, d, *J* 8.0), 6.59 (1H, d, *J* 8.0), 4.12 (3H, s), 3.92 (3H, s). Found: C, 39.31; H, 3.23; N, 11.18. Calc. for $C_8H_8N_2O_5S$: C, 39.34; H, 3.30; N, 11.47%; APCI-MS: *m*/*z* 245 ($(M + H)^+$).

4-Methylthio-7-methoxysulfonyl-2,1,3-benzoxadiazole (SO_2OMe/SMe). SO_2OMe/F (19 mg, 0.082 mmol) was dissolved in acetonitrile (2 ml). After the addition of 15% sodium methanethiolate solution (42 μl), the mixture was stirred at room temperature for 30 minutes. The reaction mixture was evaporated to dryness under reduced pressure, and the residue was chromatographed on silica gel with dichloromethane–hexane (2 : 1) to afford SO_2OMe/SMe (8.8 mg, 41%) as a yellow powder, mp: 167 °C. δ_H 8.03 (1H, d, *J* 8.0), 7.07 (1H, d, *J* 8.0), 4.00 (3H, s), 2.73 (3H, s). APCI-MS: *m*/*z* 261 ($(M + H)^+$).

Computational methods

Because of the size of the molecule, it was necessary to use semi-empirical methods in this study. All calculations were performed by means of a NEC PC-9821 Ls13. Semi-empirical AM1 and PM3 calculations were carried out using the WinMOPAC ver. 1.0 package (Fujitsu, Chiba, Japan). Several starting geometries were used for the geometry optimization to ensure that the optimized structure corresponds to a global minimum. All geometries were completely optimized (keyword PRECISE, equivalent to GNORM = 0.01 and SCFCRT = 1.D-8) by the eigenvector following routine (keyword EF). The increase of the barrier to rotation of peptide linkage was corrected for No. 1, 2, 16, 19, 21, 23, 28, 30, 33, 34, 42 and 65 (keyword MMOK).

Acknowledgements

The authors thank Dr Chang-Kee Lim, MRC toxicology unit University of Leicester, for his valuable suggestions and discussion.

References

1 K. Imai, T. Toyo'oka and H. Miyano, *Analyst*, 1984, **109**, 1365.
2 Y. Okura, M. Kai and H. Nohta, *J. Chromatogr. B*, 1994, **659**, 85.
3 C. Dejong, G. J. Hughes, W. E. Van and K. J. Wilson, *J. Chromatogr.*, 1982, **241**, 345.
4 N. Seiler, T. S. Glenewinkel and H. H. Schneider, *J. Chromatogr.*, 1973, **84**, 95.
5 A. J. Boulton, P. B. Ghosh and A. R. Katritzky, *J. Chem. Soc. B*, 1966, 1004.
6 K. Imai and Y. Watanabe, *Anal. Chem. Acta*, 1981, **130**, 377.
7 T. Toyo'oka, T. Suzuki, Y. Saito, S. Uzu and K. Imai, *Analyst*, 1989, **114**, 413.
8 T. Toyo'oka and K. Imai, *Anal. Chem.*, 1984, **56**, 2461.
9 K. Imai, T. Toyo'oka and Y. Watanabe, *Anal. Biochem.*, 1983, **128**, 413.
10 S. Udenfriend, S. Stein, P. Bohlen, W. Dairman, W. Leimgruber and M. Weogele, *Science*, 1972, **178**, 871.
11 H. Nakamura and Z. Tamura, *Anal. Chem.*, 1980, **52**, 2087.
12 M. Roth, *Anal. Chem.*, 1971, **43**, 880.
13 E. M. Kosower, *Acc. Chem. Res.*, 1982, **15**, 259.
14 G. Jones II, W. R. Jackson, C. Choi and W. R. Bergmark, *J. Phys. Chem.*, 1985, **89**, 298.
15 J. A. V. Gompel and G. B. Schuster, *J. Phys. Chem.*, 1989, **93**, 1292.
16 A. Takadate, T. Masuda, C. Murata, A. Isobe, T. Shinohara, M. Irikura and S. Goya, *Anal. Sci.*, 1997, **13**, 753.
17 H. Matsunaga, T. Santa, T. Iida, T. Fukushima, H. Homma and K. Imai, *Analyst*, 1997, **122**, 931.
18 R. Saito, T. Hirano, H. Niwa and M. Ohashi, *J. Chem. Soc.*, *Perkin Trans. 2*, 1997, 1711.
19 S. Uchiyama, T. Santa, T. Fukushima, H. Homma and K. Imai, *J. Chem. Soc.*, *Perkin Trans. 2*, 1998, 2165.
20 L. P. Hammett, *J. Am. Chem. Soc.*, 1937, **59**, 96.
21 H. H. Jaffe, *Chem. Rev.*, 1953, **53**, 191.
22 C. Hansch, A. Leo and R. W. Taft, *Chem. Rev.*, 1991, **91**, 165.
23 M. J. S. Dewar, E. G. Zoebisch, E. F. Healy and J. J. P. Stewart, *J. Am. Chem. Soc.*, 1985, **107**, 3902.
24 J. J. P. Stewart, *J. Comput. Chem.*, 1989, **10**, 209.
25 J. J. P. Stewart, *J. Comput. Chem.*, 1989, **10**, 221.
26 J. J. P. Stewart, *J. Comput. Chem.*, 1990, **11**, 543.
27 R. Karaman, J. T. L. Huang and J. L. Fry, *J. Comput. Chem.*, 1990, **11**, 1009.
28 A. Ponti and A. Gamba, *Gazz. Chim. Ital.*, 1997, **127**, 151.
29 D. Lancet and I. Pecht, *Biochemistry*, 1977, **16**, 5150.
30 H. Heberer and H. Matschiner, *J. Prakt. Chem.*, 1986, **328**, 261.
31 W. Rettig, *Angew. Chem.*, *Int. Ed. Engl.*, 1986, **25**, 971.
32 S. F. Forgues, C. Vidal and D. Lavabre, *J. Chem. Soc.*, *Perkin Trans. 2*, 1996, 73.
33 K. Imai, S. Uzu, K. Nakashima and S. Akiyama, *Biomed. Chromatogr.*, 1993, **7**, 56.
34 P. Prados, T. Fukushima, T. Santa, H. Homma, M. Tsunoda, S. Al-Kindy, S. Mori, H. Yokosu and K. Imai, *Anal. Chim. Acta*, 1997, **344**, 227.
35 T. Toyo'oka, T. Suzuki, Y. Saito, S. Uzu and K. Imai, *Analyst*, 1989, **114**, 1233.
36 L. D. Nunno, S. Florio and P. E. Todesco, *J. Chem. Soc. C*, 1970, 1433.
37 G. Gubitz, R. Wintersteiger and R. W. Frei, *J. Liq. Chromatogr.*, 1984, **4**, 839.
38 S. Uzu, S. Kanda, K. Imai, K. Nakashima and S. Akiyama, *Analyst*, 1990, **115**, 1477.

Paper 8/08010K